Published in final edited form as:
J Comp Neurol. 2011 June 1; 519(8): 1580–1596. doi:10.1002/cne.22587.

Major Isoform of Zebrafish P0 Is a 23.5 KDa Myelin Glycoprotein Expressed in Selected White Matter Tracts of the Central Nervous System

Qing Bai[1,2], **Ming Sun**[3,4], **Donna B. Stolz**[3,4], and **Edward A. Burton**[1,2,5,6,7,*]

[1]Pittsburgh Institute for Neurodegenerative Diseases, University of Pittsburgh School of Medicine, Pittsburgh, Pennsylvania

[2]Department of Neurology, University of Pittsburgh School of Medicine, Pittsburgh, Pennsylvania

[3]Center for Biological Imaging, University of Pittsburgh School of Medicine, Pittsburgh, Pennsylvania

[4]Department of Cell Biology and Physiology, University of Pittsburgh School of Medicine, Pittsburgh, Pennsylvania

[5]Department of Microbiology and Molecular Genetics, University of Pittsburgh School of Medicine, Pittsburgh, Pennsylvania

[6]Geriatric Research, Education and Clinical Center, Pittsburgh VA Healthcare System, Pittsburgh, Pennsylvania

[7]Department of Neurology, Pittsburgh VA Healthcare System, Pittsburgh, Pennsylvania

Abstract

The zebrafish *mpz* gene, encoding the ortholog of mammalian myelin protein zero, is expressed in oligodendrocytes of the zebrafish central nervous system (CNS). The putative gene product, P0, has been implicated in promoting axonal regeneration in addition to its proposed structural functions in compact myelin. We raised novel zebrafish P0-specific antibodies and established that P0 is a 23.5 kDa glycoprotein containing a 3 kDa N-linked carbohydrate moiety. P0 was localized to myelin sheaths surrounding axons, but was not detected in the cell bodies or proximal processes of oligodendrocytes. Many white matter tracts in the adult zebrafish CNS were robustly immunoreactive for P0, including afferent visual and olfactory pathways, commissural and longitudinal tracts of the brain, and selected ascending and descending tracts of the spinal cord. P0 was first detected during development in pre-myelinating oligodendrocytes of the ventral hindbrain at 48 hours postfertilization (hpf). By 72 hpf, short segments of longitudinally oriented P0-immunoreactive myelinating axons were seen in the hindbrain; expression in the spinal cord, optic pathways, hindbrain commissures, midbrain, and peripheral nervous system followed. The *mpz* transcript was found to be alternatively spliced, giving rise to P0 isoforms with alternative C-termini. The 23.5 kDa isoform was most abundant in the CNS, but other isoforms predominated in the myelin sheath surrounding the Mauthner axon. These data provide a detailed account of P0 expression and demonstrate novel P0 isoforms, which may have discrete functional properties. The restriction of P0 immunoreactivity to myelin sheaths indicates that the protein is subject to stringent intracellular compartmentalization, which likely occurs through posttranslational mechanisms.

*CORRESPONDENCE TO: Edward A. Burton, 7015 BST-3, 3501 Fifth Ave., Pittsburgh PA 15217. eab25@pitt.edu.

INDEXING TERMS

mpz; P0; zebrafish; myelin; oligodendrocyte; tectum; optic nerve; olfactory tract; tectobulbar tract; glycosylation; immunoglobulin domain

Myelin, a multilamellar sheath formed by specialized glial cell membrane extensions, surrounds axons and provides an electrical insulator that allows rapid propagation of action potentials by saltatory conduction (Huxley and Stampfli, 1949; Tasaki, 1959). The important role played by myelin in the human central nervous system (CNS) is illustrated by the serious consequences of its disruption in neurological diseases such as multiple sclerosis (Waxman, 2006) and hereditary leukodystrophies (Costello et al., 2009). There is significant interest in understanding the molecular events regulating myelin formation during development and following CNS damage, since this might enable the design of treatments aiming to promote remyelination and thereby restore normal function to patients suffering from demyelinating diseases.

Myelin, formed by oligodendrocytes in the CNS, is found throughout the vertebrate subphylum from cartilaginous fish to mammals (Kirschner et al.,, 1989). The zebrafish model offers some methodological advantages for molecular and morphological studies of myelination in vivo. Zebrafish can be manipulated to be optically transparent at the developmental points during which myelination initially occurs, allowing deployment of fluorescent reporters to observe dynamic behavior of oligodendrocytes (Kirby et al., 2006), live expression profiles of genes encoding myelin proteins (Yoshida and Macklin, 2005; Jung et al., 2010), and neural-glial interactions. Zebrafish are especially well suited to high-throughput screening (Mullins et al., 1994; Amsterdam et al., 1999; Zon and Peterson, 2005), which has been exploited to isolate novel genes involved in regulating myelination (Lyons et al., 2005, 2009), in addition to chemical modifiers that could inform the development of therapeutic compounds to promote remyelination (Buckley et al., 2010b). Finally, there are well-established techniques for modulating gene expression in zebrafish (Nasevicius and Ekker, 2000; Thermes et al., 2002; Kawakami, 2004) and a number of readily available experimental resources (Sprague et al., 2006), including gene expression atlases (Mueller and Wullimann, 2005), collections of annotated clones, mutants, and transgenic lines, which might be employed for mechanistic studies (reviewed in Sager et al., 2010).

The zebrafish CNS is rich in oligodendrocytes, which express orthologs of mammalian genes involved in myelin formation, including the cytoplasmic myelin basic protein (MBP), and the tetraspan transmembrane proteolipoprotein (PLP/DM20) (Bro¨samle and Halpern, 2002; Schweitzer et al., 2006). There are, however, some interesting differences in molecular composition between fish and mammalian CNS myelin. In mammals, myelin protein zero (P0), a type 1 transmembrane glycoprotein with an extracellular immunoglobulin-like N-terminal domain, is expressed in Schwann cells of the peripheral nervous system (PNS). P0 is thought to mediate adhesion between adjacent myelin membranes through homophilic interactions in the extracellular space separating lamellae (D'Urso et al., 1990; Filbin et al., 1990), and is essential for compact myelin formation in the PNS of mammals (Giese et al., 1992). In contrast to mammals, P0 orthologs are expressed in the brain and spinal cord of teleosts, including zebrafish and trout (the trout *mpz* gene gives rise to two P0 isoforms, called intermediate proteins 1 and 2, IP1/IP2) (Waehneldt and Jeserich, 1984; Bro¨samle and Halpern, 2002). Loss of P0-like proteins from CNS myelin is specific to mammals and is postulated to allow more compact myelin formation (Schweitzer et al., 2006), although the short intracellular domain of zebrafish P0

may allow closer approximation of myelin membrane than in mammalian PNS myelin, where the intracellular domain of P0 is comparatively large (Luo et al., 2007).

In addition to its role in compact myelin formation, P0 may have other functions in the teleost CNS, most intriguingly in axonal regrowth. Following optic nerve crush injury, zebrafish retinal ganglion cell axons regenerate over long distances to reinnervate their original targets in the optic tectum and diencephalon, and become myelinated, allowing restoration of visual function (reviewed in Becker and Becker, 2007). This contrasts sharply with the situation in humans, where CNS axonal lesions rarely show signs of recovery. These species-specific differences in axonal regeneration and remyelination are determined by properties of fish neurons and the tissue environment of the CNS (Bernhardt, 1999). Inhibitory myelin components and glial scar formation that prevent axonal growth in mammalian CNS are significantly less prominent in the fish CNS (Wanner et al., 1995; Becker and Becker, 2002). In addition, zebrafish glia express axonal growth-promoting cell surface molecules (Bernhardt, 1999). The *mpz* (myelin protein zero) transcript encoding P0 is robustly upregulated in oligodendrocytes along the entire afferent visual pathway to the tectum following optic nerve injury (Schweitzer et al., 2003). Upregulation commences before axonal regrowth is under way and lasts until remyelination is complete. It has been suggested that oligodendroglial P0 may play an important role in axonal regeneration and reinnervation of the tectum (Schweitzer et al., 2003).

These interesting and potentially important properties of zebrafish P0 have been inferred from studies examining the *mpz* mRNA transcript. Zebrafish myelin proteins of similar size to trout IP1 and IP2 have been detected by sodium dodecyl sulfate-polyacrylamide gel electrophoresis (SDS-PAGE) of myelin preparations (Morris et al., 2004; Avila et al., 2007), and may crossreact with antibodies to trout IP2 (Morris et al., 2004). However, zebrafish P0 has not been characterized, partly owing to the lack of specific and reliable antibody markers. The purpose of this study was to generate anti-P0 antibodies that specifically detect the zebrafish protein, and which could be employed in order to determine the basic biochemical properties, subcellular localization, and adult and developmental expression patterns of P0.

MATERIALS AND METHODS

Zebrafish

Experiments were carried out in accordance with Institutional Animal Use and Care Committee regulations and approvals. Adult stocks of strain AB* zebrafish were maintained at 28.5°C and euthanized by deep tricaine anesthesia followed by exposure to ice-cold water.

Generation of P0 antisera

Synthesis of peptides, immunization of animals and collection of sera were outsourced (Sigma, St. Louis, MO). P0-specific peptides 1 (extracellular; CPEVSFTWHYRPDGAK) and 2 (intracellular; CKGKGKEGSQQKQRI) were conjugated to keyhole limpet hemocyanin for immunization. After obtaining preimmunization serum, two New Zealand white rabbits were immunized with each peptide according to the following schedule. On day 0:200 μg peptide in complete Freund's adjuvant; on days 14, 28, 42, 56, and 70: 100 μg peptide in incomplete Freund's adjuvant. Serum was collected at days 49, 63, 77, and 84. Enzyme-linked immunosorbent assay showed that peptide 2 yielded a 100-fold higher titer of specific antibody (1:500,000) than peptide 1 (1:5,000).

Affinity purification of P0 antibody

Antibody to peptide 1 or 2 was affinity-purified on a column generated by coupling 2 mg peptide to AminoLink Plus Resin (Thermo, Rockford, IL), yielding 90–95% coupling efficiency. Nine mL serum obtained at day 84 of the immunization protocol was passed over the column. After washing in 5 volumes of phosphate-buffered saline (PBS), pH 7.2, bound antibodies were recovered from the column using 0.1M glycine, pH 2.7. The eluted protein fractions were neutralized in 1M Tris, pH 8.8, and analyzed by SDS-PAGE and Coomassie stain. Fractions containing purified antibody were pooled, dialyzed against PBS at 4°C overnight using a dialysis cassette (Slide-A-Lyzer, Thermo), and concentrated using centrifugal filter units (Microcon; Millipore, Billerica, MA). Purified antibody was stored at −80°C in PBS, 0.1% NaN_3.

Antibody characterization

Primary antibodies used in this study are listed in Table 1. Detailed characterization of antibodies to zebrafish myelin P0 is described in the Results. Zebrin II monoclonal antibody was originally raised against a homogenate of cerebellum and lateral line lobe from *Apteronotus leptorhynchus* (brown ghost knifefish) (Brochu et al., 1990). The antibody recognizes a single 36 kDa band on western blots of *Apteronotus* or rat brain homogenate. The cognate antigen has been identified as aldolase C by cDNA expression library screening, and confirmed by zebrin II antibody showing identical labeling patterns in the cerebellum as an independent aldolase C antibody and aldolase C mRNA (Ahn et al., 1994). Zebrin II antibody specifically labels cerebellar Purkinje cells in multiple mammalian and fish species, including zebrafish (Lannoo et al., 1991).

Western blot

Brain tissue from 5-month-old AB strain zebrafish was homogenized in RIPA buffer (50 mM Tris pH 8.0, 150 mM NaCl, 1% NP-40, 5 mM EDTA, 0.5% sodium deoxycholate, and 0.1% SDS); insoluble debris was removed by centrifugation at 21,000g at 4°C for 20 minutes; 50 μg of protein from the resulting supernatant was loaded per lane on 15% SDS-PAGE gel. Transfer to PVDF membrane (Immun-Blot, Bio-Rad, Hercules, CA) was carried out as described (Bai et al., 2006); for incubation in different primary antibodies, the membrane was divided into strips following transfer. P0 antibody was diluted 1:2,000 in PBS 10% nonfat milk and incubated at 4°C overnight. Horseradish peroxidase (HRP)-conjugated antirabbit secondary antibody (Southern Biotech, Birmingham, AL) was diluted 1:10,000 and detected by chemiluminescence (Amersham ECL Plus, GE, Piscataway, NJ). For peptide competition assays, 1 μL purified P0 antibody was preincubated with 20 (μmol peptide 1 or peptide 2 in 100 μL PBS at 37°C for 2 hours, following which antibody-peptide mixtures were centrifuged at 16,000g for 20 minutes at 4°C. The supernatant was removed and combined with PBS, 10% nonfat milk to a final dilution of 1:2,000. For deglycosylation assays, 32 **(**μg brain homogenate protein was preincubated at 37°C for 1 hour with or without 1,000 units of PNGase F (New England Biolabs, Ipswich, MA) in a total volume of 20 μL, before loading on an SDS-PAGE gel for western blotting as described above.

Immunohistochemistry

Immunohistochemistry was carried out as previously described (Bai et al., 2007; Bai and Burton, 2009). Briefly, dissected adult fish brains or whole larvae were fixed in 4% paraformaldehyde (PFA), followed by cryoprotection in PBS-sucrose. Cryosections (15 (μm) were preincubated in 3% H_2O_2, then incubated overnight at 4°C with primary P0 antibody diluted 1:500 in carrier buffer (PBS, 1% goat serum, 1% BSA). After washes in carrier buffer, sections were incubated with affinity-purified biotinylated antirabbit IgG(H +L) secondary antibody (1.5 mg/mL; Vector Laboratories, Burlingame, CA) diluted 1:200 in

carrier buffer, followed by HRP-avidin-biotin complexes (Vectastain, Vector Laboratories). Histochemical staining using NovaRed (Vector Laboratories) was followed by counterstaining in Mayer's hematoxylin (Sigma). Identical procedures were employed for immunofluorescence experiments, except that Alexa-488 antimouse and Alexa-555 antirabbit secondary antibodies were employed and H_2O_2 preincubation and histochemical reaction were omitted. Zebrin II primary antibody (Brochu et al., 1990) was diluted 1:400 for immunofluorescence labeling. For lipid removal, slides were passed through an ascending alcohol series into xylenes, incubated in xylenes for 2 × 5 minutes, then passed through a descending alcohol series back into PBS before H_2O_2 preincubation was commenced.

Immunoelectron microscopy

Samples were fixed in 2% PFA, followed by cryoprotection in PBS-sucrose. Ultrathin sections (70–100 nm) were mounted on Formvar-coated copper grids, then washed three times with PBS and three times with PBS containing 0.5% bovine serum albumin and 0.15% glycine (PBG buffer), followed by a 30-minute incubation with 5% normal goat serum in PBG. Sections were labeled with P0 antibody (1:100) in PBG for 1 hour, washed 5 times with PBG, then incubated with goat antirabbit 10 nm colloidal gold (1:25) at room temperature for 1 hour (GE). Sections were washed three times in PBG, three times in PBS, then fixed in 2.5% glutaral-dehyde in PBS for 5 minutes, washed two times in PBS, then washed six times in ddH_2O. Sections were poststained in 2% neutral uranyl acetate, for 7 minutes, washed three times in ddH_2O, stained 2 minutes in 4% uranyl acetate, then embedded in 1.25% methyl cellulose. Labeling was observed on a JEOL JEM 1011 electron microscope (Peabody, MA) at 80 kV and images were taken using a side-mount AMT 2k digital camera (Advanced Microscopy Techniques, Danvers, MA).

Image acquisition and processing

Light microscopy images were acquired using an Olympus BX-51 microscope and Olympus DP70 digital camera using the same exposure and color balance settings for each picture of a series. Images of the entire midbrain were generated by joining two photomicrographs using Adobe Photoshop (San Jose, CA) in order to enable the entire midbrain and diencephalon to be shown in each single panel. Confocal images were acquired using an Olympus IX-71 confocal microscope with Fluoview software. Laser settings were chosen to avoid saturation. Multipanel figures were assembled and annotated using Adobe Photoshop; brightness adjustments were made where necessary to match background brightness between pictures of each image series.

Reverse-transcription polymerase chain reaction (RT-PCR) and 3′RACE

Total RNA from whole adult zebrafish brains was subjected to reverse transcription, primed with either oligo-dT or a 3′RACE primer (RLM-RACE, Ambion, Austin, TX), using SuperScript III (Invitrogen, Carlsbad, CA). PCR amplification of *mpz* from first-strand cDNA was carried out using primers exon 1F (5′-TGA CCT GCG GGG AGA TCA GA-3′) and either exon 7R (5′-AAT GAA GGG TGG GGA TGG GAG G-3′) or exon 6R (5′-ATA AGA ACC CTG CCC TGC CC-3′). 3′RACE was carried out using *mpz*-specific forward primers exon 3F (5′-CCA TTC GGC TGC TGG TGT TT-3′) or exon 4F (5′-ATT ATT GGT GTA GTG TTG GG-3′), and a RACE adapter primer. PCR products were cloned in pGEM-T (Promega, Madison, WI) and sequenced. Sequences were aligned and compared using the AlignX implementation of the ClustalW algorithm. Sequences of novel *mpz* transcript variants 3, 2, and 4 were deposited in GenBank (http://www.ncbi.nlm.nih.gov/genbank/), accession numbers: HQ645214, HQ645215, HQ645216.

RESULTS

Development and characterization of novel antibodies against zebrafish P0

We verified the open reading frame of the *mpz* transcript encoding P0 by sequencing cDNA cloned by RT-PCR from adult zebrafish brain (not shown). We identified potentially antigenic peptide immunogens from the deduced translation of the consensus cDNA sequence. Using the candidate immunogen sequences as probes, available zebrafish protein databases were interrogated by BLAST, allowing selection of two peptides that were highly specific for P0, corresponding to amino acids 51–66, within the predicted extracellular immunoglobulin-like domain (peptide 1), and amino acids 189–203 at the predicted intracellular C-terminus (peptide 2) (Fig. 1A). Antisera raised against each of these peptides were tested on western blots of adult zebrafish whole brain lysate (Fig. 1B). Both antisera recognized a protein migrating at ≈23 kDa, which was not recognized by preimmune serum (a faint band of approximately this size was recognized by preimmune serum for peptide 1). Antiserum against peptide 2 also recognized an additional protein of 26 kDa nonspecifically; affinity purification of peptide 2 antiserum yielded an antibody preparation that recognized only the 23 kDa band. Preincubation of affinity-purified peptide 2 antibody with peptide 2 prevented its recognition of the 23 kDa protein, whereas preincubation of affinity-purified peptide 2 antibody with peptide 1 at the same concentration did not. These data show that affinity-purified antibody to peptide 2 specifically recognized an epitope from the C-terminus of zebrafish P0, confirming that the 23 kDa species is P0. We next examined the specificity of peptide 2 antibody in immunohistochemical applications. In adult zebrafish brain sections, peptide 2 antibody labeled white matter tracts. An example is shown in Figure 1C, which demonstrates specific labeling of tectal laminae containing myelinated axons. Preincubation of the antibody with peptide 2 abolished immunohistochemical labeling, whereas preincubation with peptide 1 at the same concentration did not. This shows that the antibody specifically recognized an epitope derived from the C-terminus of zebrafish P0 in tissue sections. Immunoelectron microscopy confirmed that the antibody recognized an antigen localized within myelin sheaths (Fig. 1D). Together, these data show that the novel antibody employed in this study specifically recognizes myelin P0; we subsequently refer to the affinity-purified peptide 2 antibody preparation as “P0 antibody.”

Myelin P0 is a 23.5 kDa glycoprotein

The availability of a specific antibody allowed us to carry out an initial biochemical characterization of P0 (Fig. 2). Western blot hybridization showed that P0 derived from brain lysate migrated as a single protein species; by interpolation from a best fit curve relating the molecular mass standards to their electrophoretic mobility, we estimate that P0 is ≈23.2–23.5 kDa. We next investigated N-glycosylation of P0. Preincubation of brain lysate with peptide:N-glycosidase F (PNGase F), an amidase that cleaves between asparagine and the innermost N-acetyl-glucosamine (GlcNAc) residue of the oligosaccharide chain of N-linked glycoproteins, altered the electrophoretic mobility of P0, which migrated at 20.5 kDa following PNGaseF treatment (Fig. 2A). This mobility shift demonstrates the presence of N-linked carbohydrate chains totaling ≈3 kDa. The consensus “sequon” or target sequence for N-glycosylation is N-X-S or N-X-T, where X is any residue except for proline. Although the predicted extracellular domain of P0 contains seven asparagine residues, only one of these, N114, is located within a consensus N-glycosylation site (N-G-T) (Fig. 2B), suggesting that there is a single 3 kDa carbohydrate moiety. The open reading frame of the *mpz* transcript encodes a 203 amino acid protein of 22.1 kDa, which is larger than the P0 protein we detected following deglycosylation. However, as expected for a transmembrane protein, the presence of an N-terminal signal peptide was predicted with >99% probability by three different algorithms, SignalP (Emanuelsson et al., 2007), SPEPLip (Fariselli et al., 2003), and PrediSi (Hiller et al., 2004). The signal peptide

cleavage site is most likely located between residues 17 and 18, or 21 and 22 (Fig. 2C). This suggests that mature P0 has 182–186 amino acids and a molecular mass of 20.1–20.5 kDa following deglycosylation, in close agreement with our western blot data (Fig. 2D).

Expression pattern of P0 in the adult CNS

We next examined P0 expression in the adult zebrafish CNS. Serial sections through the entire brains of four zebrafish were labeled immunohistochemically to detect P0. Data from these experiments are illustrated in Figures 3, 4, 5, 6 and summarized below; neuroanatomical annotation follows the published nomenclature (Wullimann et al., 1996). P0 immunoreactivity was exclusively associated with myelinated axons; there was no evidence of P0 expression in the proximal processes or perinuclear cytoplasm of oligodendrocytes in any of the sections examined.

Telencephalon (Fig. 3)—P0 was expressed at the medial and dorsolateral margins of the olfactory bulbs, at the formation of the medial and lateral olfactory tracts, which were immunoreactive for P0 throughout their caudal extent into the telencephalon, including fibers from the olfactory tracts that were seen to terminate in fan-like arborizations in the adjacent dorsal telencephalon. The medial and lateral forebrain bundles, and fibers within the central zone of the dorsal telencephalic area, also showed strong P0 immunoreactivity, but there was little expression of P0 elsewhere in the telencephalon. Ventral to the telencephalon, the optic nerves were strongly immunoreactive for P0; robust histochemical signal for P0 was also evident in myelinated fibers of the optic chiasm and optic tracts.

Mesencephalon and diencephalon (Fig. 4)—P0 was expressed in the caudal continuation of the afferent visual pathways, with robust immunoreactivity evident in the ventral and dorsal optic tracts as they coursed dorsally to reach the tectum. Within the tectum, P0 expression was observed in the optic stratum, the major afferent visual lamina of the tectum, and in the central white stratum, which gives rise to the major efferent tracts from the tectum. Bundles of P0-immunoreactive fibers arising from the central white stratum were seen traversing the periventricular lamina of the tectum, coalescing in the lateral mesencephalic tegmentum to form the tectobulbar tract. Both the uncrossed and crossed tectobulbar tracts, and the ansulate commissure (forming the crossed tract), were strongly labeled by the P0 antibody. P0 was also localized to many of the major commissural tracts, including the postoptic commissure and the tectal commissure. P0 was expressed in fibers throughout the tegmentum and torus semcircularis of the mesencephalon, such that individual tracts were mostly not discernable. However, robust P0 expression was distinguishable from surrounding structures in several diencephalic tracts. The horizontal commissure showed dense labeling throughout its course, from its rostral commissure in the ventral hypothalamus to the dorsal projection of the associated tract further caudally. Similarly, fibers of the pretectomamillary tract showed strong P0 immunoreactivity throughout their course from the pretectal region to the mammillary bodies in the inferior lobe of the hypothalamus. Interestingly, some of the most strongly P0-immunoreactive fibers from this tract appeared to terminate in the adjacent diffuse nucleus rather than the mammillary body.

Rhombencephalon (Fig. 5)—P0 expression in the cerebellum was more apparent rostrally than caudally. Within the medial and lateral divisions of the cerebellar valvulae, the caudal lobe and the body of the cerebellum, distinct bundles of P0-immunoreactive fibers were present at, and in some cases appeared to arise from, the interface between the molecular and granule cell layers (Fig. 6A, black arrows). Double label immunofluorescence to detect P0 and Zebrin II, a marker for Purkinje cells, excluded the possibility that these P0-immunoreactive fibers were Purkinje cell axons (Fig. 6B). Bundles of P0-expressing fibers

were also dispersed through the granule cell layer of the medial division of the valvulae, and in the granular eminences that form part of the vestibulolateral lobe (Fig. 6A, white arrows). Within the caudal lobe (also part of the vestibulolateral lobe) and rostral part of the body of the cerebellum, numerous dispersed single neurites were P0-immunoreactive throughout the neuropil of the molecular layer (Fig. 6B). These fibers ran perpendicularly to the projection of the Purkinje cell arborizations (Fig. 6D). It seems likely that P0-immunoreactive fibers within the cerebellum represent efferent projections from eurydendroid cells or afferent inputs from the anterior cerebellar tract, which was also P0-immunoreactive.

The medulla oblongata (Fig. 5) showed widespread P0 expression, consistent with the numerous myelinated tracts that traverse this section of the hindbrain. However, some tracts showed significant differences in labeling intensity from the majority of myelinated axons, allowing their anatomical delineation. The crossed tectobulbar tract was visible as a well-defined bundle of intensely P0 immunoreactive fibers, running in the ventral medulla near the midline, from the rostral extent of the medulla to approximately the level of cranial nerve VIII. More lateral P0-immunoreactive bundles may represent the uncrossed tectobulbar tract. The sensory root of cranial nerve VII was intensely P0-immunoreactive along its course, from its medial projection at the level of the anterior lateral line nerves, through its caudal pathway dorsal to the rhombencephalic ventricle, to its termination within the facial lobe (Fig. 6C). Similarly, the descending root of cranial nerve V was visible as a strongly stained fiber tract in the ventrolateral medulla in several sections, and fibers contributing to cranial nerve X were seen as robustly immunoreactive bundles coursing laterally in more caudal sections. The peripheral portions of cranial nerves VIII and X were also strongly P0-immunoreactive (Fig. 6G,H), confirming that P0 is expressed in the PNS in addition to CNS myelin.

Although myelinated axons within numerous tracts were strongly P0-immunoreactive as indicated, there were some notable exceptions. P0 expression was not apparent in the sheaths surrounding the Mauthner axons in sections examined at multiple levels of the medulla and spinal cord (Fig. 6D–F). In addition, immunoreactivity within the adjacent medial longitudinal fasciculus was weak rostrally and absent caudally. Finally, the spinal cord showed strong P0 expression in the ventral part of the lateral funiculus and the dorsal funiculus, and intermediate expression levels in fibers running through the gray matter of the dorsal and ventral horns. However, P0 immunoreactivity was not detected in the ventral funiculus or the dorsal part of the lateral funiculus. Since these tracts contain heavily myelinated fibers, the absence of P0 immunoreactivity was a surprise, and the question arose whether absent labeling was attributable to poor antibody penetration into dense myelin. Consequently, we removed lipids from the sections using xylene as a solvent (see Materials and Methods) before commencing immunohistochemical labeling. Lipid solubilization strongly enhanced P0-immunoreactive signal in labeled tracts throughout the CNS, but did not alter the pattern of immunoreactivity, with the following exceptions. First, immunoreactivity in the peripheral segments of the cranial nerves was disproportionately enhanced by xylene pre-treatment. Second, removal of lipids revealed P0 epitopes in the dorsal part of the lateral funiculus, allowing robust labeling by the antibody; this pretreatment also revealed weak staining in the ventral funiculus (Fig. 6K,L). However, the fibers in the medial longitudinal fascicle and the sheaths of the Mauthner axons remained unlabeled, even after xylene pretreatment.

Together, these findings show that P0 expression in the adult zebrafish CNS is localized to white matter tracts, as predicted. However, certain myelinated tracts showed particularly strong immunoreactivity, whereas others showed little or no labeling, suggesting that the epitope recognized by the antibody is targeted to selected tracts and is not expressed as a constitutive component of CNS myelin.

Developmental expression of P0

Next we examined the developmental expression pattern of P0 (Fig. 7). Previous work has shown that expression of the *mpz* transcript occurs in two phases: initially, between 16–24 hours postfertilization, mRNA expression is detected in rhombomeres of the developing hindbrain and the rostral spinal cord (Schweitzer et al., 2003; Thisse and Thisse, 2004). This early expression occurs well before myelination initiates, and starts to wane after 24 hpf. By 48 hpf, a few distinct cells in the ventral hindbrain, which are located in the area of initial myelination, and are presumably oligodendrocytes, show *mpz* expression (Bro¨samle and Halpern, 2002; Schweitzer et al., 2003). Between 48 hpf and 96 hpf, more robust mRNA expression becomes apparent in oligodendrocytes of the developing hindbrain, in addition to the midbrain and spinal cord.

We did not detect P0 in the CNS before 48 hpf by either immunohistochemistry or indirect immunofluorescence, within tissue sections or whole mount specimens (not shown). We conclude that P0 expression during the early phase of *mpz* mRNA expression does not occur at sufficient levels to enable detection of the protein by these techniques. After 48 hpf, expression of P0 followed that of its transcript. P0 was first detected in the cytoplasm (Fig. 7A; white arrow) and short slender processes (black arrows) of one to three cells in the ventral hindbrain at 48 hpf. These may represent premyelinating oligodendrocytes. By 72 hpf, thicker longitudinally arranged linear areas of P0 immunoreactivity, suggestive of myelinating axons, were visible in one or two sections within the ventral hindbrain (Fig. 7B; black arrows). By 96 hpf, P0 expressing fibers in the ventral hindbrain were more prominent and clearly arranged in bundles, although immunoreactivity in the cytoplasm of cells was no longer visible (Fig. 7C; black arrows). Between 5 and 8 days postfertilization (dpf), P0 expression became more robust and widespread in the ventral hindbrain; in addition to longitudinally oriented P0-immunoreactive fiber bundles, laterally oriented commissural fibers began to show P0 expression by 6 dpf and were robustly immunoreactive by 8 dpf (Fig. 7D; longitudinal fibers labeled with black arrows, commissural fibers with white arrows). Cross-sections of the developing hindbrain at 14 dpf showed the ventromedial position of the labeled tracts and commissures, and revealed P0 expression in developing cranial nerve roots as they exited the ventral brainstem (Fig. 7E, arrow).

The spinal cord started to show discrete cells with short slender processes exhibiting P0 immunoreactivity between 5 and 6 dpf, similar to the cells seen in the hindbrain at 48 hpf. By 10 dpf, the rostral spinal cord showed P0-expressing tracts in ventral and dorsolateral positions (Fig. 7F). No P0 expression was visible in association with Mauthner axons at this point; however, faint immunoreactivity in developing ventral nerve roots exiting the cord could be seen on some sections (Fig. 7G, black arrow). By 24 dpf, robust P0 immunoreactivity was visible in fiber bundles running along the cord (Fig. 7H), which in cross-section were seen to reside in the ventral and dorsal funiculi and in the dorsal part of lateral funiculus, in addition to the medial longitudinal fascicle. Robust immunoreactivity was also visible in spinal ventral nerve roots at this point (Fig. 7J, arrow).

The visual pathways showed weak expression of P0 in the optic nerves, chiasm and optic tracts in the diencephalon at 7 dpf (Fig. 7K–M). This was followed by expression in the optic tracts as they reach the midbrain, the first P0 expression in the mesencephalic optic pathways being noted at 10 dpf (Fig. 7M). By 28 dpf, bundles of robustly P0-immunoreactive fibers were seen curving into the optic tectum from the optic tracts (Fig. 7N). P0 expression was seen in the deep layers of the tectum after 20 dpf, and by 28 dpf bundles of P0-immunoreactive fibers forming the developing tectobulbar tract were seen crossing the periventricular layer of the tectum; at this point, numerous longitudinal fibers were labeled within the mesencephalic tegmentum (Fig. 7O). No expression of P0 was seen

in the telencephalon or olfactory system by 28 dpf (Fig. 7P), and we conclude that the onset of expression in this part of the forebrain occurs later than 4 weeks postfertilization.

mpz is alternatively spliced to generate P0 isoforms

In view of the unexpected finding that P0 immunoreactivity was not present in the myelin sheath of the Mauthner axon, or in selected other spinal cord tracts, we examined the possibility that alternative splicing gives rise to different P0 isoforms that are not detected by the antibody used for these studies. In order to detect novel sequences at the 3′ end of the transcript (which encodes the C-terminal epitope to which the antibody was raised) we employed rapid amplification of 3′ cDNA ends (3′RACE; Fig. 8A). Amplification of RACE adapter-primed cDNA from adult brain, using primers hybridizing to exon 3 or exon 4 of *mpz*, generated a single major product and a slightly smaller product of low abundance. The bands were cloned and sequenced; the major product, which we designated transcript variant 1 (TV1), encodes the known P0 isoform, from which the peptide antigens were derived. The minor 3′RACE product (TV2) arises from use of an alternative splice acceptor site further 3′ in the terminal exon (which we have designated exon 7, see below) (Fig. 8B). However, 3′RACE did not reveal any novel exons.

Trout *mpz* is alternatively spliced to generate two isoforms, the larger of which (IP2) contains an additional 29 amino acids at the C-terminus of the protein (Lanwert and Jeserich, 2001). IP2 contains a highly conserved EKK motif that is also present in chicken and rat P0. Using a degenerate probe sequence, GA($^{A}/_{G}$)AA($^{A}/_{G}$)AA($^{A}/_{G}$), encoding this conserved amino acid triplet, we searched the genomic sequence following exon 5 of the zebrafish gene. One of the matching sequences, lying almost 6 kb 3′ of exon 5, occurred within an open reading frame with predicted homology to trout IP2. The putative exon (which we have designated exon 6) was flanked at its 5′ end by a splice acceptor consensus sequence, tccctctctttccag/GCT. We designed primers to the sequence of the novel putative exon and were able to amplify *mpz* transcripts from brain cDNA in which splicing occurred between exons 5 and 6, as opposed to the exon 5–7 splicing event that occurs in TV1 (Fig. 8B,C). The phase of the splicing event was appropriate to continue the P0 open reading frame from exon 5. In addition, we found a minor exon 6-containing transcript, in which an alternative splice acceptor within intron 5 gave rise to a transcript containing intronic sequences including a CA repeat. We designated the exon 6-containing transcripts TV3 and TV4 (Fig. 8B). We did not detect transcripts containing both exon 6 and exon 7. 3′RACE using primers specific to TV3 and TV4 suggested that exon 6 is an alternative terminal exon.

We cloned and sequenced the open reading frames for each of the four transcript variants and deduced the amino acid sequences of the P0 isoforms they encode. The major form of P0 encoded by TV1 shares closest homology to trout IP1, whereas the most abundant exon 6-containing mRNA, TV3, encodes a protein with homology to trout IP2 (Fig. 8D). TV2 and TV4 were of much lower abundance than TV1 and TV3, and their importance is unclear. The antibody used in this study was raised against an amino acid sequence present in the isoform encoded by the major transcript TV1. The C-terminal 2 amino acids of this sequence are replaced in the putative P0 isoforms encoded by TV2, 3, and 4, and it is possible that this disrupts the cognate epitope recognized by the antibody. Consequently, it is possible that the antibody to peptide 2 only recognizes the P0 isoform encoded by TV1. We therefore asked whether the antibody raised against peptide 1, whose sequence is predicted to be present in all four P0 isoforms, would recognize other P0 molecules. Affinity-purified peptide 1 antibody recognized the 23.5 kDa P0 species in western blot of brain lysate, similar to peptide 2 antibody. However, after longer exposure of both blots, the antibody to peptide 1 also recognized a 26 kDa protein of low abundance, which was not

recognized by the antibody to peptide 2 (Fig. 8E). The P0 isoform encoded by TV3 is predicted to be 26 kDa in size, presuming similar signal peptide cleavage and glycosylation to the major 23.5 kDa isoform; these observations are compatible with the presence of an IP2-like isoform of P0. Finally, we asked if peptide 1 antibody labeled tracts that were not immunoreactive for P0 using peptide 2 antibody, since this might imply that the unlabeled regions expressed the 26 kDa P0 isoform. Unfortunately, affinity-purified peptide 1 antibody did not perform well on tissue sections. Despite employing several different antigen retrieval techniques, we were only able to obtain weak signal on IHC analyses of CNS tissue, and moderate labeling of the sheath surrounding the Mauthner axon (Fig. 8F). It seems likely that, similar to trout, the zebrafish MA sheath expresses an IP2-like isoform of P0. However, these initial findings await confirmation using further antibodies, including those raised against the unique sequence of the zebrafish IP2-like isoform encoded by TV3.

DISCUSSION

Our data indicate that P0 is expressed in the zebrafish brain as a major 23.5 kDa glycoprotein, with a 3 kb carbohydrate moiety, similar to trout IP1 (Jeserich and Waehneldt, 1987). In a recent study, zebrafish P0 from zebrafish PNS and CNS myelin preparations was reported to be 24 kDa in size, comprising a 7 kDa carbohydrate group and 17 kDa protein (Avila et al., 2007). This large carbohydrate modification is unusual, and more than twice the size of the 3 kDa oligosaccharide that we found in zebrafish and which was reported for both trout IP1 and IP2 (Jeserich and Waehneldt, 1987). The reasons for the differences between our findings and the published data (Avila et al., 2007) are not immediately clear; the immunoblots previously reported showed several P0-immuno-reactive bands in each lane, and it is possible that the antibodies used in the prior study crossreacted with other P0 isoforms or other proteins. These observations suggest that the zebrafish 23.5 kDa P0-specific antibodies described here will be useful for future studies.

The cellular distribution of P0 in vivo appeared to be tightly regulated. After initial expression of P0 in the cytoplasm of cells during early myelination in several brain regions, P0 immunoreactivity was exclusively localized to myelin sheaths. Similar observations were made in trout, where antibodies to the 36 kDa dehydrogenase component of myelin (36K) stained oligodendrocyte cell bodies, whereas antibodies to IP1 and IP2 labeled only myelin (Jeserich and Waehneldt, 1986). In contrast to the mbp transcript, *mpz* mRNA does not appear to be transported along oligodendrocyte processes; *mpz* transcript is detected abundantly in the cytoplasm surrounding the oligodendrocyte nucleus but not further distally in the cell (Bro¨samle and Halpern, 2002; Schweitzer et al., 2003; Bai et al., 2007). Consequently, the striking cellular distribution of P0 is likely attributable to posttranslational mechanisms, such as transport of mature P0 to sites of myelin formation or turnover, or impaired stability/ enhanced degradation of P0 when not associated with the myelin sheath. Recent work has shown that ectopic expression of myelin proteins within oligodendrocytes may have deleterious consequences (Lyons et al., 2009). A mutation in *kif1b*, encoding a kinesin motor implicated in transport of myelin protein mRNAs, caused abnormal accumulation of MBP and the 36 kDa dehydrogenase in oligodendrocyte cell bodies. This was associated with reduced myelination of axons and the formation of ectopic myelin-like structures that did not ensheathe axons (Lyons et al., 2009). Although the mechanisms of protein localization differ substantially between MBP/36K and P0, it is possible that myelin proteins share a common requirement for strict subcellular compartmentalization in order to ensure normal function.

The temporal and spatial coordinates at which we observed P0 expression commence during development are consistent with electron microscopic studies showing that myelination initiates in the ventral hindbrain at 72– 96 hpf (Bro¨samle and Halpern, 2002; Buckley et al.,

2010a). The earliest P0 expression we detected at 48 hpf was likely present in premyelinating oligodendrocytes, since the protein was detected in cytoplasm rather than myelin sheaths. P0 was subsequently expressed in myelin of the spinal cord, optic pathways, mesencephalon, and cranial nerves in a stereotyped sequence, mirroring the topological expression pattern of the *mpz* transcript and other genes involved in myelin formation (Bro¨samle and Halpern, 2002). Earlier events during development are of interest, since *mpz* is expressed in rhombomeres of the developing hindbrain from 16–24 hpf (Schweitzer et al., 2003). We did not detect P0 at these earlier timepoints using a variety of techniques. It is possible that before 48 hpf, alternative splicing produces a protein isoform that is not recognized by our antibody; consequently, it will be of interest to examine whether alternative splicing of *mpz* changes during early development. Alternatively, *mpz* cRNA probes might cross-hybridize with another neural tube transcript early during development, in which case expression of the protein reported here may accurately reflect the expression pattern of the transcript.

We anticipated that P0 would be expressed in myelinated tracts throughout the adult brain and spinal cord. Our studies confirmed that P0 is restricted to myelin sheaths in the CNS, and the antibody labels the majority of white matter tracts and will therefore be useful as an immunohistochemical marker for myelin. However, we were surprised that not all myelinated tracts showed P0 expression. Variability between labeling intensity in different tracts could potentially reflect differences in degrees of myelination in many brain areas. However, this could not account for findings in the medial longitudinal fascicle or Mauthner axons. These tracts are heavily myelinated and were readily identifiable in multiple sections, but their myelin sheaths showed little or no P0 expression, even after lipid solubilization sufficient to reveal P0 epitopes in other initially immunonegative CNS regions. Our studies showed evidence that the 3′ end of the *mpz* transcript is subject to alternative splicing, giving rise to P0 isoforms with divergent C-termini. The antibody used for our study was raised against a peptide corresponding to the C-terminus of the 23.5 kDa isoform. The peptide was conjugated at its N-terminus for immunization; consequently, its C-terminus would have been most accessible for immune recognition. It is possible that the dominant epitope recognized by peptide 2 antiserum includes the C-terminal 2 amino acids of the peptide sequence, which are absent from P0 isoforms other than the 23.5 kDa glycoprotein. This could disrupt recognition of P0 isoforms encoded by TV2, 3, or 4 by peptide 2 antibody, potentially accounting for myelinated tracts that were not immunoreactive using this antibody. In support of this possibility, studies using an antibody raised against a P0 peptide whose sequence is predicted to be shared by all four putative isoforms showed evidence of a 26 kDa IP2-like isoform, which was not recognized by the C-terminus antibody. These observations are compatible with previous SDS-PAGE analysis of purified myelin proteins from zebrafish lateral line nerve (Morris et al., 2004; Avila et al., 2007). Two zebrafish proteins with molecular masses approximating those of trout IP1 and IP2 were detected in the published studies, and we predict that these correspond to the proteins encoded by *mpz* TV1 and TV3. Trout IP2 is expressed in the myelin sheath of Mauthner axons in addition to other white matter tracts (Jeserich and Waehneldt, 1986), whereas expression of IP1 (which is more closely related to the 23.5 kDa zebrafish P0 isoform) has not been reported in detail in trout. Our initial data suggest that the zebrafish Mauthner axon myelin sheath expresses a P0 isoform other than the 23.5 kDa protein, the 26 kDa IP2-like protein being an obvious candidate. Unfortunately peptide 1 antibody, which recognized the 26 kDa isoform on western blot, does not perform well on tissue sections. Consequently, clarification of the expression patterns of P0 isoforms other than the 23.5 kDa glycoprotein will require development of new antibodies.

The functional roles of the alternative P0 cytoplasmic tails encoded by the alternatively spliced forms of *mpz* are uncertain. The cell adhesive properties of trout IP1 could be

enhanced in an in vitro assay by altering its cytoplasmic domain (Lanwert and Jeserich, 2001), demonstrating that alterations to the C-terminus of the protein can exert significant functional modulation. Clues regarding possible functions of different isoforms might arise from their spatial and temporal expression patterns. For example, our data suggest that there is developmental regulation of P0 isoforms in the spinal cord: the 23.5 kDa isoform was expressed strongly in the medial longitudinal fascicle and ventral funiculus during development, but showed little expression in these locations in the adult. This developmental switch could be related to axonal growth. For example, myelin associated with axons that exceed a certain size threshold during development might require structural or signaling functions provided by alternative cytoplasmic P0 domains, potentially explaining the apparently preferential absence of immunoreactive signal for the 23.5 kDa isoform from tracts containing larger axons in the adult CNS. Another important question is whether the P0 isoform profile is altered in the visual pathways or spinal cord following crush injury. The *mpz* transcript is strikingly upregulated in these situations, well before remyelination takes place, and P0 may play an important role in axon regeneration (Schweitzer et al., 2003). It will be of considerable interest to establish whether specific isoforms of P0 are upregulated at different points during the regenerative process. It is possible that changes to the structure of the P0 cytoplasmic domain mediate specific functions that allow oligodendrocytes to promote axonal regrowth and then remyelination under postinjury conditions.

Acknowledgments

The authors thank Dr. Richard Hawkes (University of Calgary) for kindly providing the Zebrin II antibody used to generate Figure 6B,D.

Grant sponsor: NINDS; Grant number: NS058369; Grant sponsor: Ethel Vincent Charitable Trust.

Abbreviations

C	Central canal of spinal cord
Cans	Ansulate commissure
CC	Cerebellar crest
CCe	Body of cerebellum
Chor	Horizontal commissure
CM	Mammillary body
Cpop	Postoptic commissure
Ctec	Tectal commissure
D	Dorsal telencephalic area
Dd	Dorsal zone of D
DH	Dorsal horn of spinal cord
DIL	Diffuse nucleus of the inferior lobe
DiV	Diencephalic ventricle
Dl	Lateral zone of D
Dm	Medial zone of D
DOT	Dorsal optic tract

DV	Descending root of cranial nerve V
EG	Granular eminence
Fd	Dorsal funiculus of spinal cord
Fl	Lateral funiculus of spinal cord
Fv	Ventral funiculus of spinal cord
Hd	Dorsal zone of periventricular hypothalamus
Hv	Ventral zone of periventricular hypothalamus
IMRF	Intermediate reticular formation
LCa	Caudal lobe of cerebellum
LFB	Lateral forebrain bundle
LLF	Lateral longitudinal fasciculus
LOT	Lateral olfactory tract
LVII	Facial lobe
LX	Vagal lobe
MA	Mauthner axon
MdO	Medulla oblongata
MFB	Medial forebrain bundle
MLF	Medial longitudinal fascicle
MOT	Medial olfactory tract
Nin	Interpeduncular nucleus
OB	Olfactory bulb
OC	Optic chiasm
ON	Optic nerve
OT	Optic tract
PLLN	Posterior lateral line nerve
PPa	Anterior parvocellular preoptic nucleus
RV	Rhombencephalic ventricle
SAC	Central white layer of TeO
SFGS	Superficial gray/fibrous layer of TeO
SGC	Central gray layer of TeO
SM	Marginal layer of TeO
SO	Optic layer of TeO
SPV	Periventricular layer of TeO
SRF	Superior reticular formation
TelV	Telencephalic ventricle
TeV	Tectal ventricle

TeO	Optic tectum
TL	Torus longitudinalis
TS	Torus semicircularis
TPM	Pretecto-mamillary tract
TTB	Tecto-bulbar tract
TTBc	Crossed tectobulbar tract
TTBr	Uncrossed tecto bulbar tract
Val	Lateral division of cerebellar valvula
Vam	Medial division of cerebellar valvula
VH	Ventral horn of spinal cord
VIIs	Sensory root of cranial verve VII
VIII	Cranial nerve VIII
VOT	Ventral optic tract
X	Cranial nerve X

LITERATURE CITED

Ahn AH, Dziennis S, Hawkes R, Herrup K. The cloning of zebrin II reveals its identity with aldolase C. Development. 1994; 120:2081–1290. [PubMed: 7925012]

Amsterdam A, Burgess S, Golling G, Chen W, Sun Z, Townsend K, Farrington S, Haldi M, Hopkins N. A large-scale insertional mutagenesis screen in zebrafish. Genes Dev. 1999; 13:2713–2724. [PubMed: 10541557]

Avila RL, Tevlin BR, Lees JP, Inouye H, Kirschner DA. Myelin structure and composition in zebrafish. Neurochem Res. 2007; 32:197–209. [PubMed: 16951904]

Bai Q, Burton EA. Cis-acting elements responsible for dopaminergic neuron-specific expression of zebrafish slc6a3 (dopamine transporter) in vivo are located remote from the transcriptional start site. Neuroscience. 2009; 164:1138–1151. [PubMed: 19755139]

Bai Q, Mullett SJ, Garver JA, Hinkle DA, Burton EA. Zebrafish DJ-1 is evolutionarily conserved and expressed in dopaminergic neurons. Brain Res. 2006; 1113:33–44. [PubMed: 16942755]

Bai Q, Garver JA, Hukriede NA, Burton EA. Generation of a transgenic zebrafish model of Tauopathy using a novel promoter element derived from the zebrafish eno2 gene. Nucleic Acids Res. 2007; 35:6501–6516. [PubMed: 17897967]

Becker CG, Becker T. Repellent guidance of regenerating optic axons by chondroitin sulfate glycosaminoglycans in zebrafish. J Neurosci. 2002; 22:842–853. [PubMed: 11826114]

Becker CG, Becker T. Growth and pathfinding of regenerating axons in the optic projection of adult fish. J Neurosci Res. 2007; 85:2793–2799. [PubMed: 17131420]

Bernhardt RR. Cellular and molecular bases of axonal regeneration in the fish central nervous system. Exp Neurol. 1999; 157:223–240. [PubMed: 10364435]

Brochu G, Maler L, Hawkes R. Zebrin II: a polypeptide antigen expressed selectively by Purkinje cells reveals compartments in rat and fish cerebellum. J Comp Neurol. 1990; 291:538–552. [PubMed: 2329190]

Bro¨samle C, Halpern ME. Characterization of myelination in the developing zebrafish. Glia. 2002; 39:47–57. [PubMed: 12112375]

Buckley CE, Marguerie A, Alderton WK, Franklin RJ. Temporal dynamics of myelination in the zebrafish spinal cord. Glia. 2010a; 58:802–812. [PubMed: 20140960]

Buckley CE, Marguerie A, Roach AG, Goldsmith P, Fleming A, Alderton WK, Franklin RJ. Drug reprofiling using zebrafish identifies novel compounds with potential promyelination effects. Neuropharmacology. 2010b; 59:149–159. [PubMed: 20450924]

Costello DJ, Eichler AF, Eichler FS. Leukodystrophies: classification, diagnosis, and treatment. Neurologist. 2009; 15:319–328. [PubMed: 19901710]

D'Urso D, Brophy PJ, Staugaitis SM, Gillespie CS, Frey AB, Stempak JG, Colman DR. Protein zero of peripheral nerve myelin: biosynthesis, membrane insertion, and evidence for homotypic interaction. Neuron. 1990; 4:449–460. [PubMed: 1690568]

Emanuelsson O, Brunak S, von Heijne G, Nielsen H. Locating proteins in the cell using TargetP, SignalP and related tools. Nat Protoc. 2007; 2:953–971. [PubMed: 17446895]

Fariselli P, Finocchiaro G, Casadio R. SPEPlip: the detection of signal peptide and lipoprotein cleavage sites. Bioinformatics. 2003; 19:2498–2499. [PubMed: 14668245]

Filbin MT, Walsh FS, Trapp BD, Pizzey JA, Tennekoon GI. Role of myelin P0 protein as a homophilic adhesion molecule. Nature. 1990; 344:871–872. [PubMed: 1691824]

Giese KP, Martini R, Lemke G, Soriano P, Schachner M. Mouse P0 gene disruption leads to hypomyelination, abnormal expression of recognition molecules, and degeneration of myelin and axons. Cell. 1992; 71:565–576. [PubMed: 1384988]

Hiller K, Grote A, Scheer M, Munch R, Jahn D. PrediSi: prediction of signal peptides and their cleavage positions. Nucleic Acids Res. 2004; 32:W375–W379. [PubMed: 15215414]

Huxley AF, Stampfli R. Evidence for saltatory conduction in peripheral myelinated nerve fibres. J Physiol. 1949; 108:315–339.

Jeserich G, Waehneldt TV. Characterization of antibodies against major fish CNS myelin proteins: immunoblot analysis and immunohistochemical localization of 36K and IP2 proteins in trout nerve tissue. J Neurosci Res. 1986; 15:147–158. [PubMed: 2421005]

Jeserich G, Waehneldt TV. Antigenic sites common to major fish myelin glycoproteins (IP) and to major tetrapod PNS myelin glycoprotein (Po) reside in the amino acid chains. Neurochem Res. 1987; 12:825–829. [PubMed: 2444896]

Jung SH, Kim S, Chung AY, Kim HT, So JH, Ryu J, Park HC, Kim CH. Visualization of myelination in GFP-transgenic zebrafish. Dev Dyn. 2010; 239:592–597. [PubMed: 19918882]

Kawakami K. Transgenesis and gene trap methods in zebrafish by using the Tol2 transposable element. Methods Cell Biol. 2004; 77:201–222. [PubMed: 15602913]

Kirby BB, Takada N, Latimer AJ, Shin J, Carney TJ, Kelsh RN, Appel B. In vivo time-lapse imaging shows dynamic oligodendrocyte progenitor behavior during zebrafish development. Nat Neurosci. 2006; 9:1506–1511. [PubMed: 17099706]

Kirschner DA, Inouye H, Ganser AL, Mann V. Myelin membrane structure and composition correlated: a phylogenetic study. J Neurochem. 1989; 53:1599–1609. [PubMed: 2795020]

Lannoo MJ, Ross L, Maler L, Hawkes R. Development of the cerebellum and its extracerebellar Purkinje cell projection in teleost fishes as determined by zebrin II immunocytochemistry. Prog Neurobiol. 1991; 37:329–363. [PubMed: 1758964]

Lanwert C, Jeserich G. Structure, heterologous expression, and adhesive properties of the P(0)-like myelin glycoprotein IP1 of trout CNS. Microsc Res Tech. 2001; 52:637–644. [PubMed: 11276116]

Luo X, Inouye H, Gross AA, Hidalgo MM, Sharma D, Lee D, Avila RL, Salmona M, Kirschner DA. Cytoplasmic domain of zebrafish myelin protein zero: adhesive role depends on beta-conformation. Biophys J. 2007; 93:3515–3528. [PubMed: 17693467]

Lyons DA, Pogoda HM, Voas MG, Woods IG, Diamond B, Nix R, Arana N, Jacobs J, Talbot WS. erbb3 and erbb2 are essential for schwann cell migration and myelination in zebrafish. Curr Biol. 2005; 15:513–524. [PubMed: 15797019]

Lyons DA, Naylor SG, Scholze A, Talbot WS. Kif1b is essential for mRNA localization in oligodendrocytes and development of myelinated axons. Nat Genet. 2009; 41:854–858. [PubMed: 19503091]

Morris JK, Willard BB, Yin X, Jeserich G, Kinter M, Trapp BD. The 36K protein of zebrafish CNS myelin is a short-chain dehydrogenase. Glia. 2004; 45:378–391. [PubMed: 14966869]

Mueller, T.; Wullimann, MF. Amsterdam. Boston; Elsevier: 2005. Atlas of early zebrafish brain development: a tool for molecular neurogenetics.

Mullins MC, Hammerschmidt M, Haffter P, Nusslein-Volhard C. Large-scale mutagenesis in the zebrafish: in search of genes controlling development in a vertebrate. Curr Biol. 1994; 4:189–202. [PubMed: 7922324]

Nasevicius A, Ekker SC. Effective targeted gene 'knockdown' in zebrafish. Nat Genet. 2000; 26:216–220. [PubMed: 11017081]

Sager JJ, Bai Q, Burton EA. Transgenic zebrafish models of neurodegenerative diseases. Brain Struct Funct. 2010; 214:285–302. [PubMed: 20162303]

Schweitzer J, Becker T, Becker CG, Schachner M. Expression of protein zero is increased in lesioned axon pathways in the central nervous system of adult zebrafish. Glia. 2003; 41:301–317. [PubMed: 12528184]

Schweitzer J, Becker T, Schachner M, Nave KA, Werner H. Evolution of myelin proteolipid proteins: gene duplication in teleosts and expression pattern divergence. Mol Cell Neurosci. 2006; 31:161–177. [PubMed: 16289898]

Sprague J, Bayraktaroglu L, Clements D, Conlin T, Fashena D, Frazer K, et al. The Zebrafish Information Network: the zebrafish model organism database. Nucleic Acids Res. 2006; 34:D581–D585. [PubMed: 16381936]

Tasaki I. Physiologic properties of the myelin sheath and of the node of Ranvier. Prog Neurobiol. 1959; 4:159–172. [PubMed: 13836984]

Thermes V, Grabher C, Ristoratore F, Bourrat F, Choulika A, Wittbrodt J, Joly JS. I-SceI meganuclease mediates highly efficient transgenesis in fish. Mech Dev. 2002; 118:91–98. [PubMed: 12351173]

Thisse, C.; Thisse, B. Fast release clones: a high throughput expression analysis. ZFIN. 2004. Available at: http://www.zfin.org

Waehneldt TV, Jeserich G. Biochemical characterization of the central nervous system myelin proteins of the rainbow trout, Salmo gairdneri. Brain Res. 1984; 309:127–134. [PubMed: 6488002]

Wanner M, Lang DM, Bandtlow CE, Schwab ME, Bastmeyer M, Stuermer CA. Reevaluation of the growth-permissive substrate properties of goldfish optic nerve myelin and myelin proteins. J Neurosci. 1995; 15:7500–7508. [PubMed: 7472501]

Waxman SG. Axonal conduction and injury in multiple sclerosis: the role of sodium channels. Nat Rev Neurosci. 2006; 7:932–941. [PubMed: 17115075]

Wullimann, MF.; Rupp, B.; Reichert, H. Neuroanatomy of the zebrafish brain. Berlin: Birkhauser; 1996.

Yoshida M, Macklin WB. Oligodendrocyte development and myelination in GFP-transgenic zebrafish. J Neurosci Res. 2005; 81:1–8. [PubMed: 15920740]

Zon LI, Peterson RT. In vivo drug discovery in the zebrafish. Nat Rev Drug Discov. 2005; 4:35–44. [PubMed: 15688071]

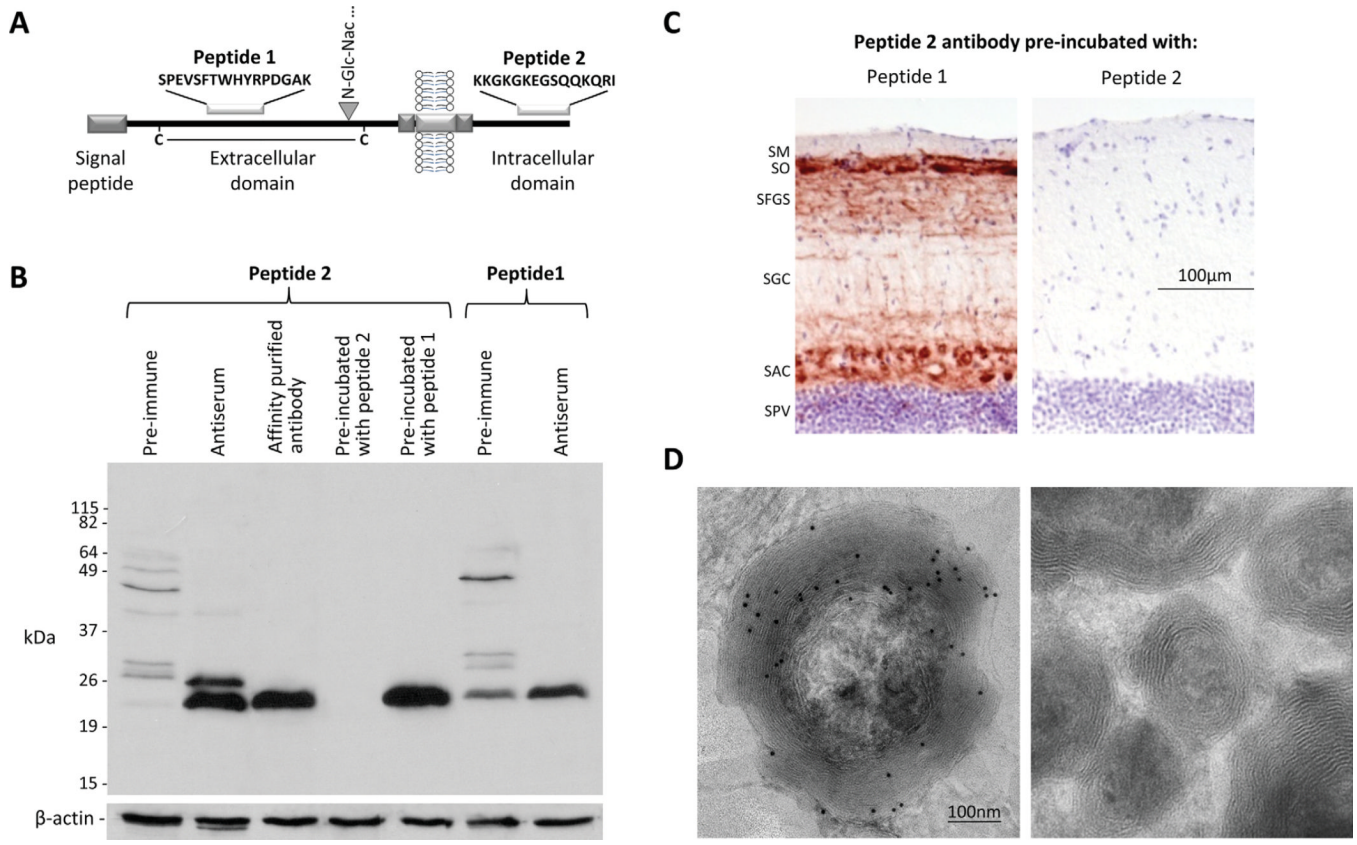

Figure 1.

Development of specific antibodies against zebrafish P0. A: The diagram shows the predicted domain organization of zebrafish P0, illustrating key features discussed in the text. The positions and sequences of the two peptides used to raise P0 antibodies are shown. B: Zebrafish whole brain lysate (50 μg protein/lane) was separated by SDS-PAGE and transferred to PVDF membrane. The resulting western blot was divided into strips, allowing each lane to be probed using a different primary antibody: 1) preimmune serum from an animal subsequently immunized with peptide 2; 2) antiserum from the same animal following immunization with peptide 2; 3) affinity-purified antibody against peptide 2 derived from the serum shown in lane 2 (this is referred to as “P0 antibody” in Figs. 2–7); 4) affinity-purified antibody shown in lane 3, preincubated with peptide 2; 5) affinity-purified antibody shown in lane 3, preincubated with peptide 1; 6) preimmune serum from an animal subsequently immunized with peptide 1; 7) antiserum from the same animal following immunization with peptide 1. After incubation with secondary antibody, the strips were reassembled into the original blot, prior to the application of chemiluminescent reagent, in order to allow direct comparison between lanes. The blot was subsequently reprobed with an antibody to β-actin in order to verify equal protein loading in each lane (bottom panel). C: Cryosections encompassing the optic tectum were labeled immunohistochemically using affinity-purified peptide 2 antibody (shown in lane 3 of panel B). The antibody was preincubated with peptide 2, containing its cognate epitope (right panel), or with peptide 1 at the same concentration, as a negative control (left panel). Bound antibody was detected using a histochemical reaction with a red product. A blue nuclear counterstain was used in order to facilitate identification of tectal laminae. The scale bar for both panels is shown in the right panel. D: Transmission electron micrographs of adult zebrafish spinal cord showing myelinated axons in cross-section. The specimen on the left was immunolabeled with

affinity-purified peptide 2 antibody (shown in lane 3 of panel B). The secondary antibody was conjugated to 10 nm colloidal gold and the specimen counterstained with uranyl acetate; immunoreactivity appears as small black circles. The panel on the right shows a control sample that was processed identically, except that primary antibody was omitted.

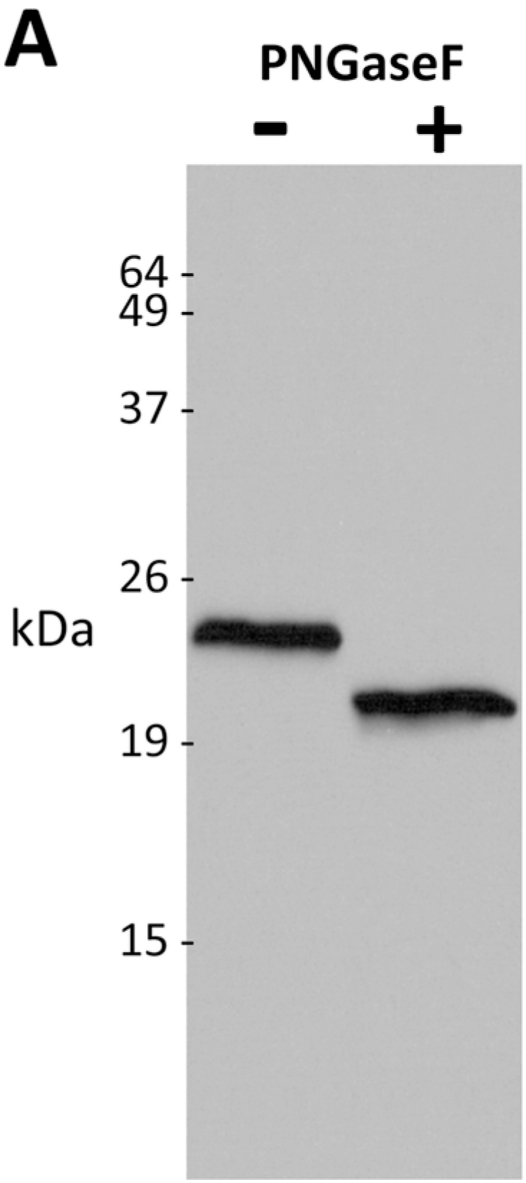

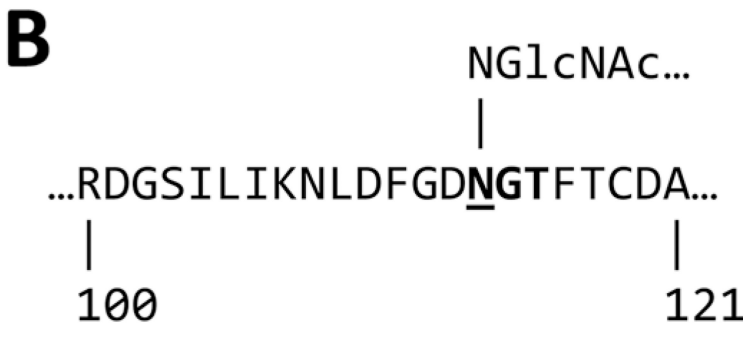

D

Signal peptide	Protein size	Mr (kDa)
1-17	186 aa	20.44
1-21	182 aa	20.05

Figure 2.

Zebrafish P0 is a 23.5 kDa glycoprotein. **A**: A western blot probed with P0 antibody. Whole adult zebrafish brain lysate (32 μg protein per lane) was incubated with (+; right lane) or without (—; left lane) PNGaseF, prior to SDS-PAGE and western transfer. **B**: A short segment of the predicted extracellular domain of P0 is shown is shown (amino acids are numbered with respect to the full open reading frame). The consensus N-glycosylation motif is shown in bold. Underlining denotes the asparagine residue to which the N-acetyl-glucosamine side chain is linked. **C**: The N terminus of P0 is shown, illustrating the predicted signa peptide cleavage sites. **D**: The table shows the size and predicted molecular mass of P0 after cleavage of the signal peptide at each of the putative cleavage sites.

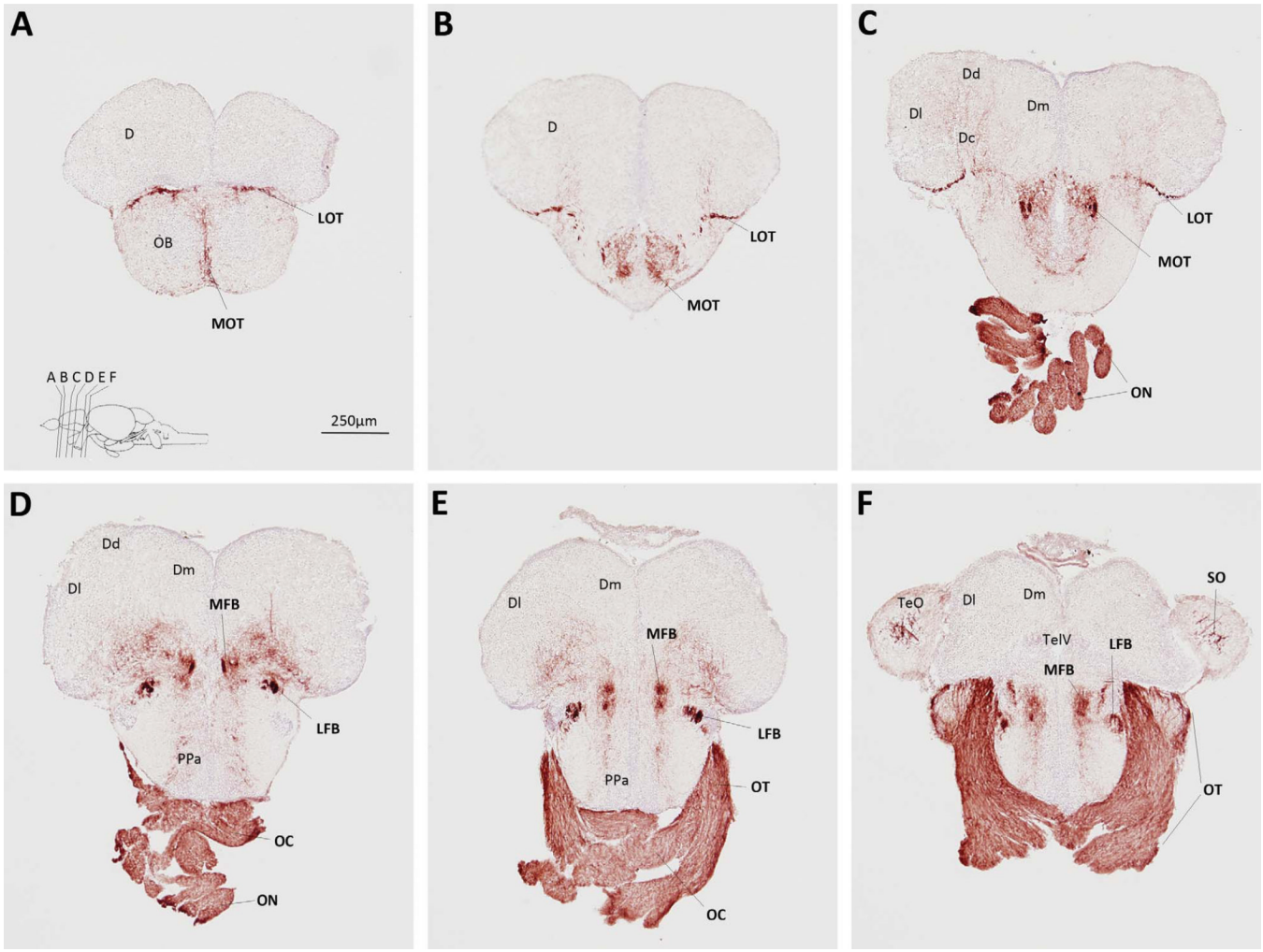

Figure 3.

Myelin P0 expression in the telencephalon, optic nerves, and adjacent structures. Transverse sections of adult zebrafish brain, from posterior olfactory bulbs to anterior tectum, were labeled using P0 primary antibody, and a histochemical reaction yielding a red product. A blue nuclear counterstain was used to facilitate identification of anatomical features. The sections, which are oriented dorsal upwards, progress in a rostrocaudal direction; their planes are indicated in the inset to **A**, which also shows the scale bar for all six panels. Anatomical landmarks are indicated on the left side of each image, and P0-immunoreactive structures are labeled in bold on the right side of each image. For anatomical annotations, please see list of abbreviations.

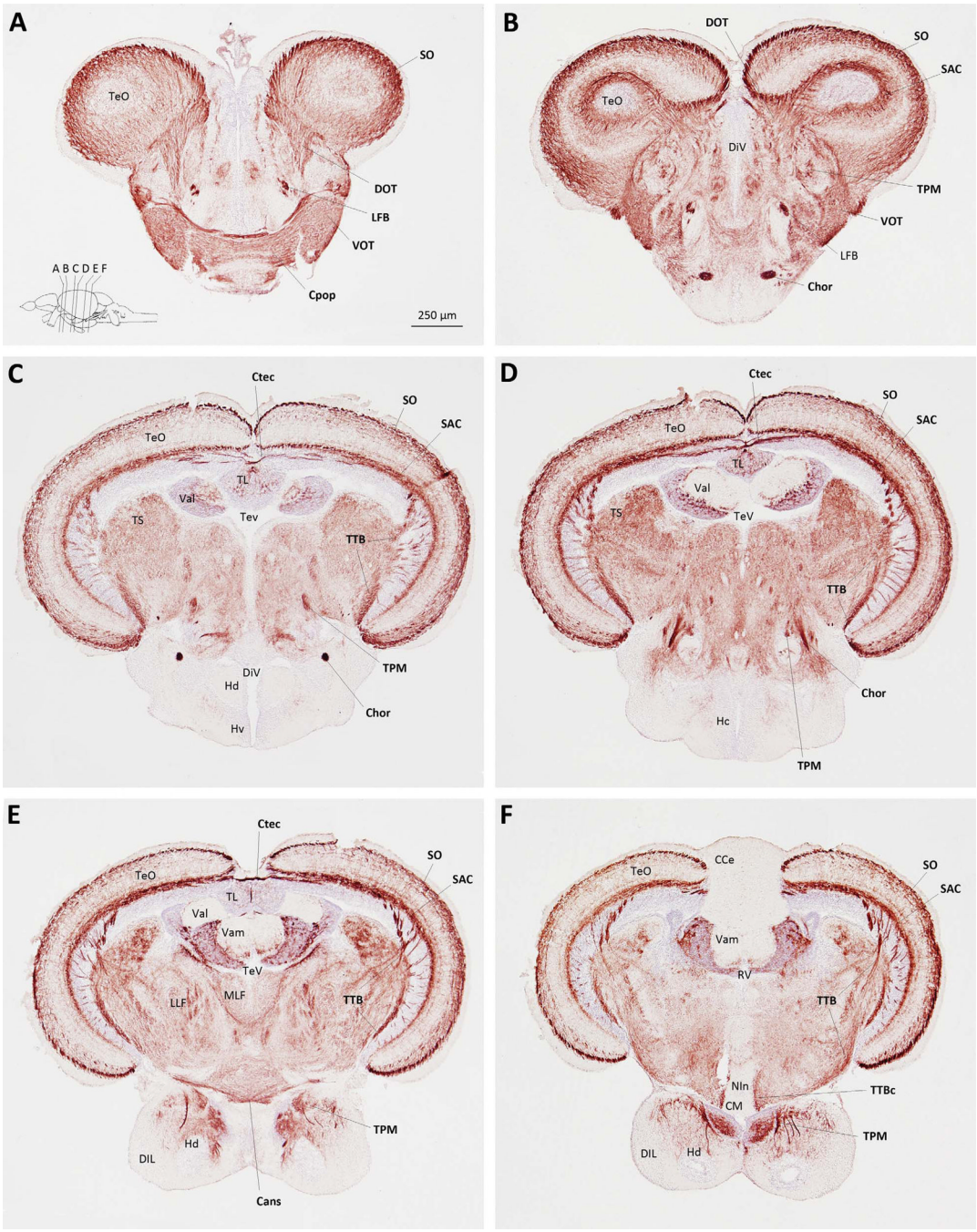

Figure 4.

Myelin P0 expression in the optic tectum, hypothalamus, and adjacent structures. Transverse sections of adult zebrafish brain, from the level of the postoptic commissure to the mammillary bodies, were labeled using the same method employed to generate Figure 3. Sections are oriented dorsal upwards and progress in a rostrocaudal direction; their planes are indicated in the inset to **A**, which also shows the scale bar for all six panels. Anatomical landmarks are indicated on the left side of each image, and P0-immunoreactive structures are labeled in bold on the right side of each image.

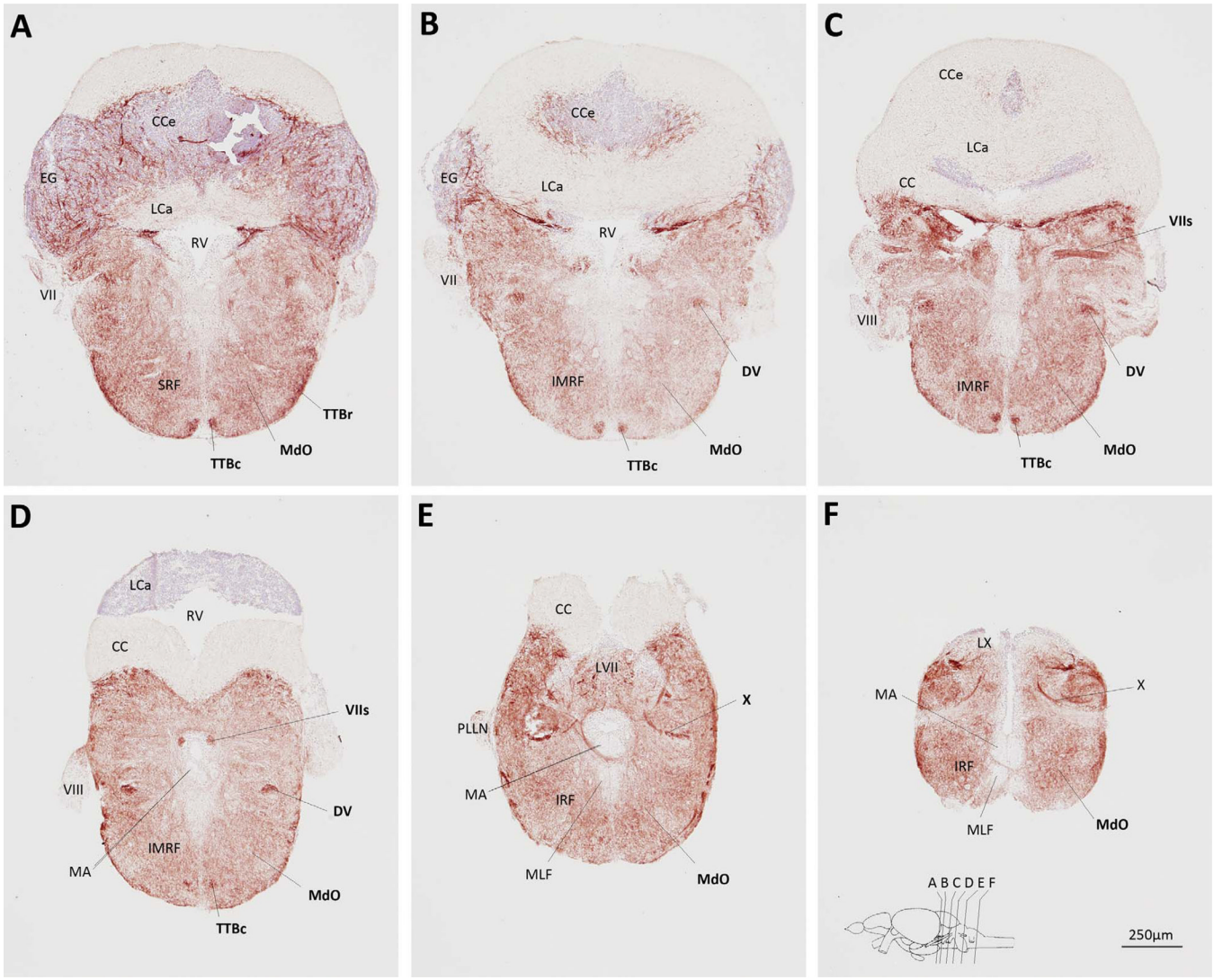

Figure 5.

Myelin P0 expression in the hindbrain. Transverse sections of adult zebrafish hindbrain were labeled using the same method employed to generate Figure 3. Sections are oriented dorsal upwards and progress in a rostrocaudal direction; their planes are indicated in the inset to **F**, which also shows the scale bar for all six panels. Anatomical landmarks are indicated on the left side of each image and P0-immunoreactive structures are labeled in bold on the right side of each image.

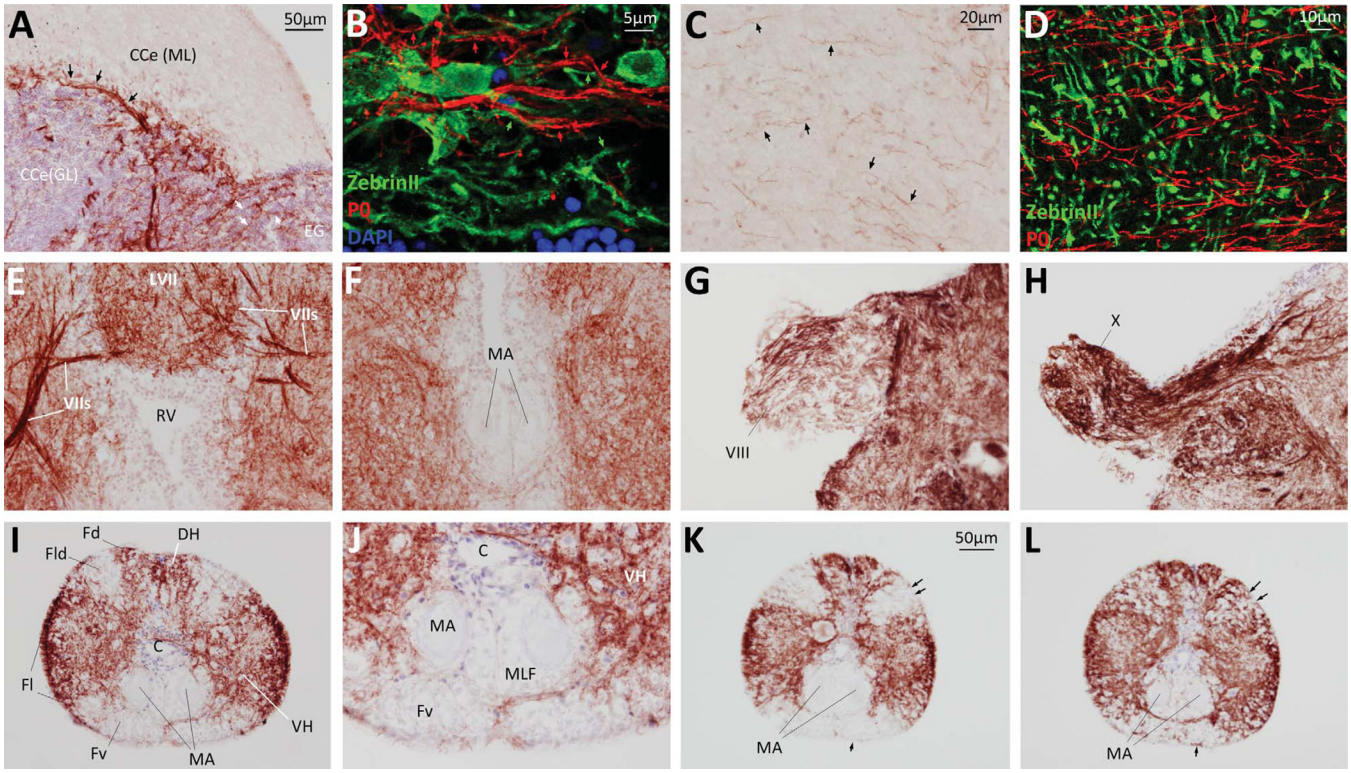

Figure 6.

Myelin P0 expression in the hindbrain, cranial nerves, and spinal cord. Transverse sections of adult zebrafish hindbrain and spinal cord were labeled by immunohistochemistry to reveal P0 (A,C,E–L), or by immunofluorescence to detect P0 (red), Zebrin II (green) and nuclei (blue) (B,D). The bar in A shows the scale for A,E–I; the bar in C shows the scale for C,J; the bar in K shows the scale for K,L. **A**: Body of cerebellum. Black arrows indicate bundles of P0-immunoreactive fibers that appear to arise from the junction between the molecular and granule cell layers. White arrows indicate P0-expressing fibers that pass through the granular eminence. **B**: A single confocal plane is shown at the junction between the molecular and granule cell layers to illustrate the relationship between P0 immunoreactive fibers (red, red arrows) and Purkinje cells and their axons (green, green arrows). Nuclei of the granule cell layer (blue) are seen at the bottom of the image. **C**: Body of cerebellum. The neuropil of the molecular layer is shown. Black arrows show examples of the numerous single P0-immunoreactive fibers passing through the molecular layer. **D**: A single confocal plane of the molecular layer is shown to illustrate the relationship between P0 immunoreactive fibers (red) and Purkinje cell dendrites (green). **E**: Dorsal medulla. **F**: Ventral medulla. **G**: Cranial nerve VIII. **H**: Cranial nerve X. **I–L**: Spinal cord. Images K,L show adjacent sections that were labeled identically, except that the section shown in panel L was pretreated to remove myelin lipids before processing for immunohistochemistry. The black arrows show the regions in Fld and Fv that show enhanced P0 immunoreactivity following lipid solubilization.

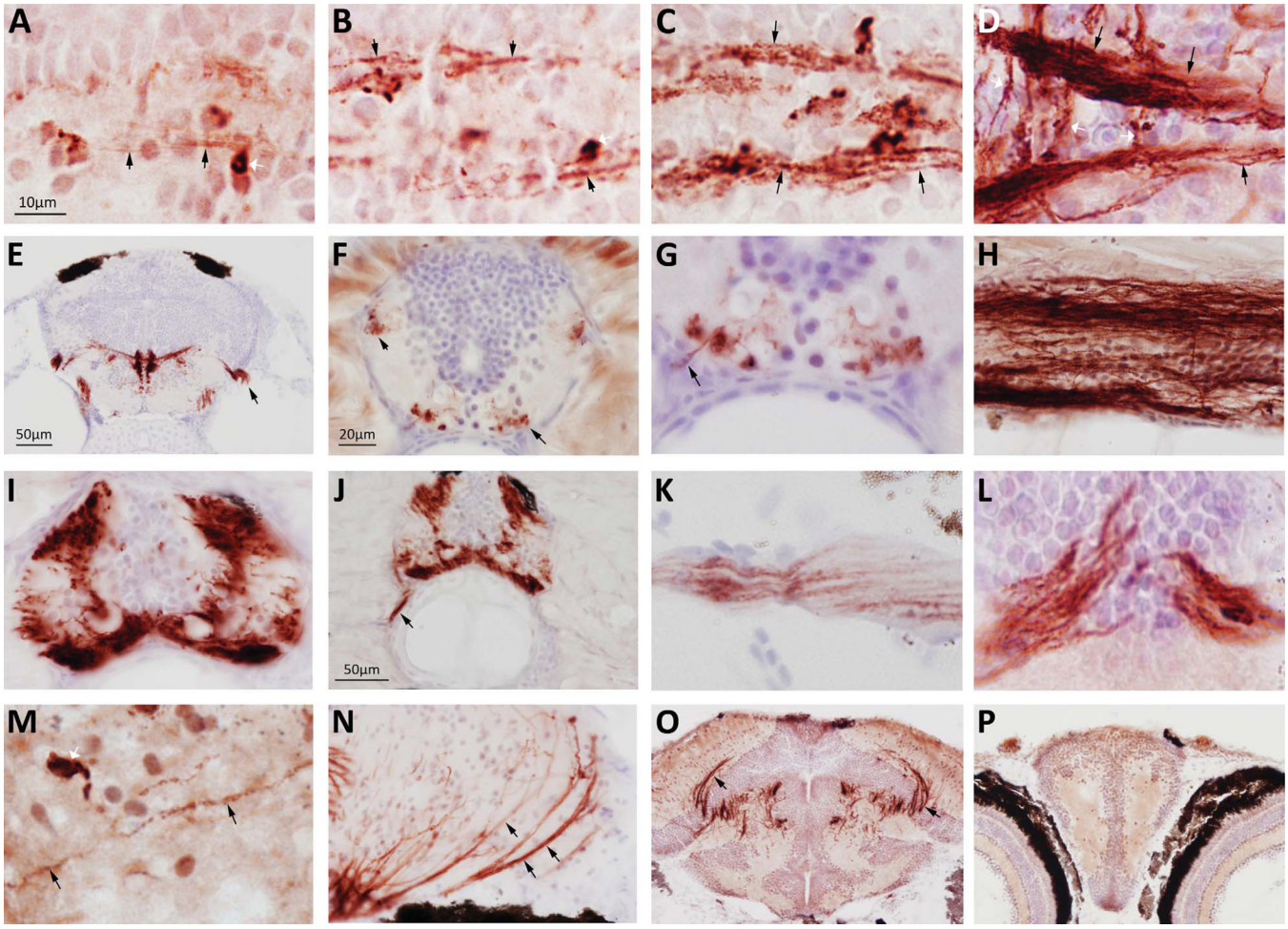

Figure 7.

Developmental expression of P0. Sections of zebrafish larvae were labeled using the same method employed to generate Figure 3, illustrating developmental P0 expression in the hindbrain (A–E), the spinal cord (F–J), the visual pathways (K–N), the mesencephalon (O), and the telencephalon (P). The scale bar for images A–D,G,K–M is shown in A; the scale bar for images E,O is shown in panel E; the scale bar for images F,H,I,N is shown in panel F; the scale bar for images J,P is shown in panel J. Horizontal sections of the ventral hindbrain are shown at: **A**: 48 hours post-fertilization (hpf); **B**: 72 hpf; **C**: 96 hpf; **D**: 8 dpf. In A, the white arrow shows a P0-immunoreactive premyelinating oligodendrocyte; the black arrows indicate fine P0-immunoreactive processes arising from this and similar cells. In B–D, black arrows indicate longitudinally arranged myelinating fibers. White arrows in D show myelinating commissural fibers. **E**: Hindbrain, transverse section, 14 dpf; arrow demarcates P0 expression in cranial nerve roots emerging from the ventral surface of the developing brainstem. **F**: Spinal cord, transverse section, 10 dpf; arrows indicate locations of P0-expressing spinal tracts. **G**: Higher-magnification view of ventral spinal cord from panel **F**, arrow indicates P0 expression in a ventral spinal nerve root. **H**: Longitudinal and I,J: transverse sections of the spinal cord, 24 dpf; arrow in J indicates P0 expression in a ventral nerve root. **K**: Optic nerve, longitudinal section at 7 dpf. **L**: Optic chiasm, transverse section at 8 dpf. **M**: Optic tectum, longitudinal section, 10 dpf; arrow indicates P0-immunoreactive processes of oligodendrocyte shown in center of panel. **N**: Optic tectum, transverse section, 24 dpf; arrows show P0-immunmoreactive fibers of optic tract entering the tectum. **O**:

mesencephalon and diencephalon, transverse section, 28 dpf. **P**: Telencephalon and eyes, transverse section, 28 dpf.

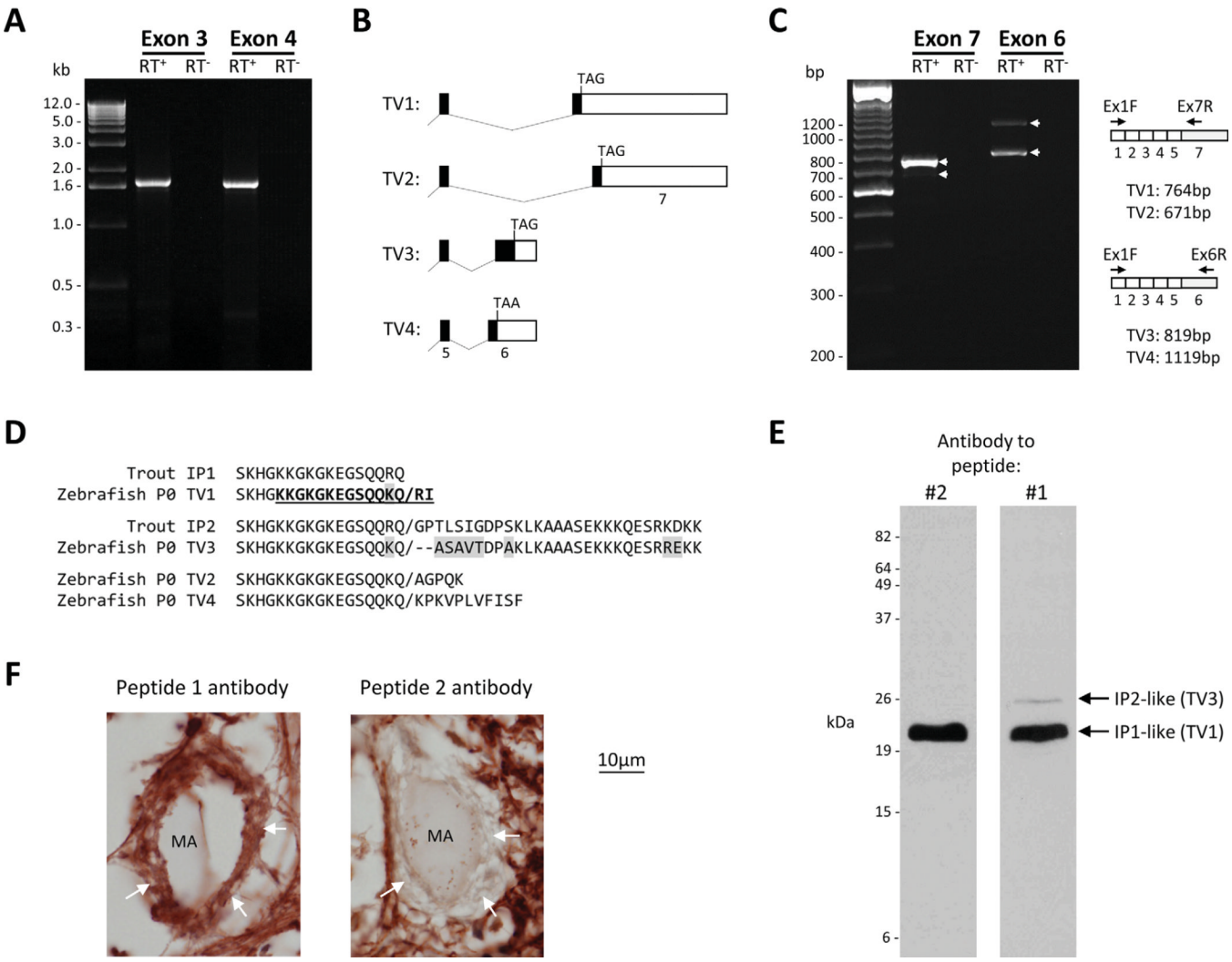

Figure 8.

Alternative splicing of *mpz* gives rise to P0 isoforms with divergent C-termini. **A**: RNA derived from adult brain was subjected to reverse transcription using a 3'RACE adapter primer (RT^+, lanes 2 and 4), or treated with buffer alone (RT^-, lanes 3 and 5). The resulting cDNA was subjected to PCR amplification using *mpz*-specific 5′ primers hybridizing to exon 3 (lanes 2 and 3) or exon 4 (lanes 4 and 5), and a 3'RACE adapter primer. Lane 1 shows a molecular marker; the sizes of the fragments (kb) are annotated to the left of the image. **B**: The diagram (not to scale) illustrates the splicing events giving rise to four *mpz* transcript variants (TV1–4). TV1 and TV2 were cloned by 3'RACE; TV3 and TV4 were identified in silico and cloned by RT-PCR (see text). **C**: RNA derived from adult brain was subjected to reverse transcription using an oligo-dT primer (RT^+, lanes 2 and 4), or treated with buffer alone (RT^-, lanes 3 and 5). The resulting cDNA was subjected to PCR amplification using *mpz*-specific primers hybridizing to exon 1 and either exon 7 (lanes 2 and 3) or exon 6 (lanes 4 and 5). Lane 1 shows a molecular marker; the sizes of the fragments (bp) are annotated to the left of the image. The schematic to the right of the gel image illustrates the exon structures of the transcripts and the sizes of the expected PCR products for each transcript variant; arrows on the gel image delineate PCR products corresponding to the four transcript variants. **D**: The sequence alignment shows the C termini of the deduced P0 protein sequences encoded by the four zebrafish *mpz* transcript

variants, and trout IP1 and IP2. The proteins encoded by *mpz* TV1 and TV3 show homology to trout IP1 and IP2, respectively. The sequence of peptide 2 used to generate the antibody used in Figures 2–7 is indicted within the sequence encoded by TV1 in bold type and underlined. Shading shows amino acid differences between the zebrafish and trout proteins. **E**: Identical western blots containing zebrafish whole brain lysate were probed using either the antibody to peptide 2 (shown in Figs. 2–7), or affinity-purified antibody to peptide 1. The additional 26 kDa band recognized by peptide 1 antibody is indicated. **F**: Photomicrographs showing high-magnification images of Mauthner axons in the ventral spinal cord, in cross-section. The myelin sheath of the Mauthner axon is indicated with white arrows. The section shown in the left panel was labeled with peptide 1 antibody (extracellular domain, sequence common to all isoforms). The section on the right was labeled with peptide 2 antibody (C-terminus, alternatively spliced). P0 immunoreactivity was revealed by a histochemical reaction with a red product.

TABLE 1

Primary Antibodies Used in This Study

Antibody	Immunogen	Source	Dilution
P0 (peptide 1)	CPEVSFTWHYRPDGAK	This study	1:500 (IHC/IF) 1:2,000 (western)
P0 (peptide 2)	CKGKGKEGSQQKQRI	This study	1:500 (IHC/IF) 1:2,000 (western)
Zebrin II	Cerebellum and lateral line lobe homogenate from *Apteronotus leptorhynchus*	Brochu et al., 1990	1:400